Synthesis and Characterization of Lanthanide Hydroxide Single-Crystal Nanowires**

Xun Wang and Yadong Li*

Nanowires represent a class of quasi-one-dimensional materials, in which carrier motion is restricted in two directions so that they usually exhibit significant photochemical, photophysical, and electron-transport properties which differ from that of bulk or nanoparticle materials.[1–11] In the last decade, many important materials have been prepared in the form of nanorods or nanowires to generate some unexpected properties[2–5] based on which, many new potential applications have been explored. For example, well-controlled and monodisperse CdSe nanorods can be used in solar cells,[2] and can form liquid-crystal phases with orientational order and positional disorder in organic solvents;[3] single-crystalline, well-defined ZnO nanowires can serve as natural resonance cavities, and well-aligned ZnO nanowire arrays may serve as room-temperature ultraviolet nanolasers.[4] Along with chemical composition and crystal structure, shape and dimensionality are now regarded as particularly important factors that influence the chemical and/or physical properties of materials.

As a consequence of their unique electronic structures and the numerous transition modes involving the 4f shell of their ions, lanthanide compounds usually have outstanding optical, electrical, and magnetic properties,[12–22] and have been widely used as high-quality phosphors,[12] up-conversion materials,[13] catalysts,[14] and time-resolved fluorescence (TRF) labels for biological detection.[15] There have been extensive studies regarding lanthanide chemistry at bulk or atomic levels,[16–19] and the synthesis of lanthanide monothiooxides,[20] lanthanide-doped oxides or sulfides, organolanthanide compounds, the complexation behavior of lanthanide ions or atoms,[16,17] and the emission phenomena from lanthanides when bound to biomolecules (including calcium-binding proteins and nucleic acids).[18,19] Very recently, the synthesis of lanthanide oxide[21] and fluoride[22] nanoparticles with enhanced luminescence and photomagnetic properties has also been reported. However, to the best of our knowledge, few studies have focused on the synthesis of nanowires or nanorods of lanthanide-related compounds. Such materials would be of great significance because of the possible novel properties induced by their reduced dimensionality. Herein, we report the synthesis of lanthanide hydroxide nanowires ($La(OH)_3$, $Pr(OH)_3$, $Nd(OH)_3$, $Sm(OH)_3$, $Eu(OH)_3$, $Gd(OH)_3$, $Dy(OH)_3$, $Tb(OH)_3$, $Ho(OH)_3$, $Tm(OH)_3$, and YbOOH) through a facile solution-based hydrothermal synthetic pathway.

The synthesis of $Ln(OH)_3$ nanowires was based on the preparation of colloidal $Ln(OH)_3$ at room temperature, with subsequent hydrothermal treatment at 180 °C for about 12 h.

Figure 1 A shows typical XRD patterns for $La(OH)_3$ nanowires. All of the reflections could be readily indexed to the hexagonal phase (space group $P63/m$ (no. 176)) of $La(OH)_3$ with lattice constants $a = 6.5470$ and $c = 3.8540$ Å (JCPDS 83-2034). Colloidal $La(OH)_3$ nanoparticles have also been characterized as the corresponding hexagonal phase of $La(OH)_3$ with broadened peaks that indicate reduced particle sizes (Figure 1 B). Similar XRD patterns to those obtained for $La(OH)_3$ nanowires and colloidal nanoparticles have also been obtained from their $Pr(OH)_3$, $Nd(OH)_3$, $Sm(OH)_3$, $Eu(OH)_3$, $Gd(OH)_3$, $Dy(OH)_3$, $Tb(OH)_3$, $Ho(OH)_3$, and $Tm(OH)_3$ counterparts, all of which exhibited hexagonal crystal structures. However, under the same conditions, the hexagonal phase of $Yb(OH)_3$ could not been obtained. The final product was found to be the monoclinic phase (space group $P21/m$ (no. 11)) of YbOOH, with lattice constants $a = 5.8700$, $b = 3.5800$, and $c = 4.2700$ Å (Figure 2).

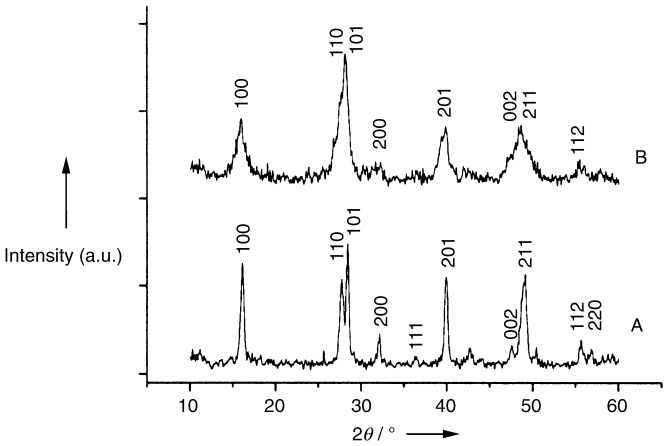

Figure 1. XRD patterns of $La(OH)_3$. A) $La(OH)_3$ nanowires; B) colloidal $La(OH)_3$.

The size and morphology of the products were further examined by transmission electron microscopy (TEM). As

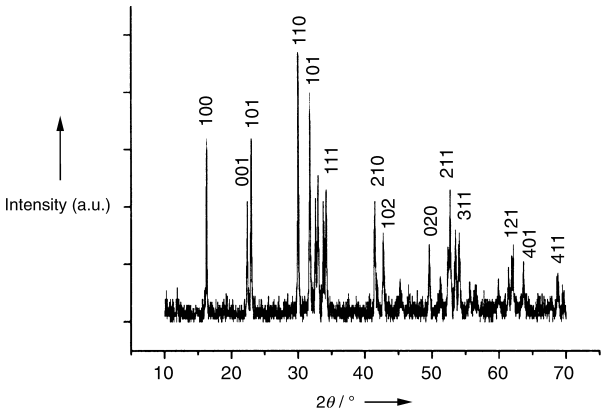

Figure 2. XRD patterns of monoclinic YbOOH.

[*] Prof. Y. Li, X. Wang
Department of Chemistry
Tsinghua University
Beijing, 100084 (P.R. China)
Fax: (+86) 10-62788765
E-mail: ydli@tsinghua.edu.cn

[**] This work was supported by the NSFC (20025102, 50028201, 20151001), the Foundation for the Author of National Excellent Doctoral Dissertation of P.R. China, and the State Key Project of Fundamental Research for nanomaterials and nanostructures.

  0044-8249/02/4124-4790 $ 20.00+.50/0

shown in Figure 3A, typical TEM images of $La(OH)_3$ nanowires display uniform morphologies with diameters of 15–20 nm and lengths up to 5 μm. Electron diffraction patterns (Figure 3B) taken form a single $La(OH)_3$ nanorod reveal the single-crystalline nature of the sample, and can be indexed as the [010] zone axis of hexagonal $La(OH)_3$, which is consistent with the XRD results presented above. High-resolution (HR)TEM images (Figure 3C) show that the nanorod is structurally uniform with an interplanar spacing is about 0.316 nm, which corresponds to the (101) plane of hexagonal $La(OH)_3$. It is interesting to observe that under controlled experimental conditions, the lighter $Ln(OH)_3$ ($La(OH)_3$, $Pr(OH)_3$, $Nd(OH)_3$, $Sm(OH)_3$, $Eu(OH)_3$, and $Gd(OH)_3$) nanowires could be prepared with high aspect ratios and uniform morphologies, whereas heavier lanthanide hydroxides ($Dy(OH)_3$, $Tb(OH)_3$, $Ho(OH)_3$, $Tm(OH)_3$ and YbOOH) usually have lower aspect ratios or less uniform morphologies when prepared under the same conditions (Table 1). Figure 3H shows a typical TEM image of $Ho(OH)_3$ nanorods with diameters of approximately 10 nm and lengths of 100–500 nm.

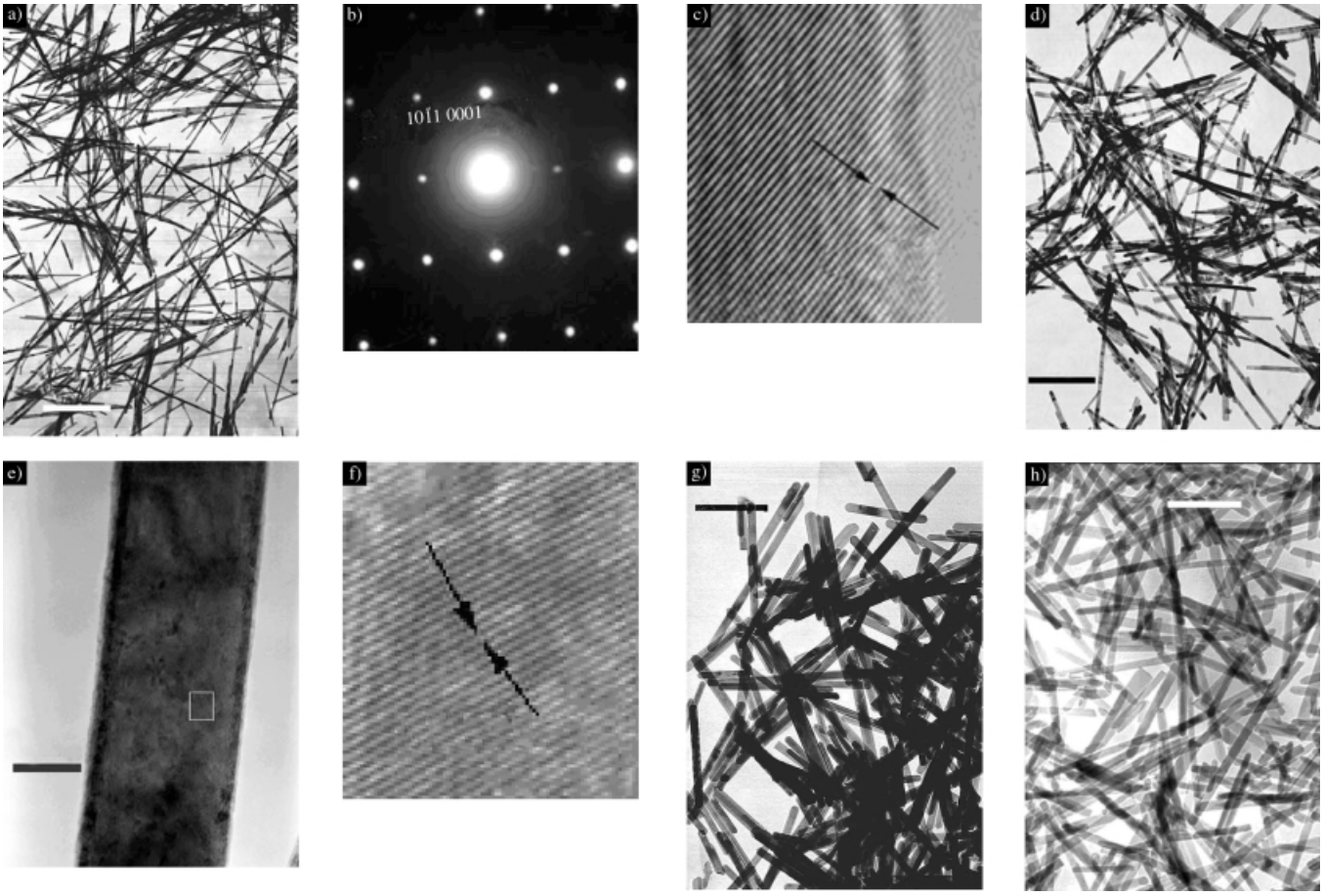

Figure 3. a) TEM image of $La(OH)_3$ nanowires (KOH, 5 mol L^{-1}, bar = 1 μm); b) Electron diffraction pattern of a single $La(OH)_3$ nanowire; c) HRTEM image of a single $La(OH)_3$ nanowire (spacing = 0.316 nm; d) TEM image of $Pr(OH)_3$ nanowires (KOH, 5 mol L^{-1}, bar = 500 nm); e) TEM image of a uniform 20 nm diameter $Pr(OH)_3$ nanowire (bar = 10 nm); f) HRTEM image of a $Pr(OH)_3$ nanowire taken from the highlighted section of (e), (spacing = 0.310 nm (101)); g) TEM image of $Eu(OH)_3$ nanowires (KOH, 5 mol L^{-1}, bar = 250 nm); h) TEM image of $Ho(OH)_3$ nanorods (at approximately pH 14, bar = 100 nm).

Table 1. Optimal experimental conditions and morphologies of lanthanide hydroxide nanowires.

Products	pH	XRD	Morphology	
			Diameter [nm]	Length [μm]
$La(OH)_3$	KOH 5 mol L^{-1}	hexagonal	15–20	2–5
$Pr(OH)_3$	KOH 5 mol L^{-1}	hexagonal	20–30	2–5
$Nd(OH)_3$	KOH 5 mol L^{-1}	hexagonal	20–30	2–5
$Sm(OH)_3$	pH 9	hexagonal	20–30	2–5
$Eu(OH)_3$	KOH 5 mol L^{-1}	hexagonal	20–30	2–5
$Gd(OH)_3$	pH 7	hexagonal	20–50	2–3
$Dy(OH)_3$	pH 14	hexagonal	40–60	0.5–1
$Tb(OH)_3$	pH 14	hexagonal	40–60	1–5
$Ho(OH)_3$	pH 14	hexagonal	~10	0.1–0.5
$Tm(OH)_3$	pH 14	hexagonal	10–20	0.5–1
YbOOH	pH 14	monoclinic	nanorods, microrods, and irregular particles coexist	

  0044-8249/02/4124-4791 $ 20.00+.50/0

Hydrothermal methods have been shown to be effective in the synthesis of nanowires, nanorods, and nanotubes.[10,11] In contrast to synthetic strategies, such as the vapor-liquid-solid (VLS) or template-confined methods, the adopted synthetic method has no catalyst to serve as the energetically favorable site for the absorption of reactant molecules (VLS), and has no template to guide the directional growth of nanowires (template-confined). Thus, it is reasonable to imagine that the driving force for the anisotropic growth of $Ln(OH)_3$ nanowires derives from the inherent crystal structure of $Ln(OH)_3$ materials and their chemical potential in solution.

The majority of the lanthanide hydroxide nanowires that were prepared possessed a hexagonal crystal structure, similar to that of ZnO, which is well-known to exhibit anisotropic growth.[4] However, under the adopted experimental conditions, those hydroxides with the smallest metal-ion centers, that is, YbOOH (which is formed here instead of the hexagonal $Yb(OH)_3$) and $Lu(OH)_3$ (which does not form nanowires) are obtained with monoclinic crystal structures. In addition to this change, the tendency to grow along a certain direction has been weakened to some extent, so that the heavier lanthanide hydroxides usually have lower aspect ratios and less uniform morphologies (Table 1).

The influence of chemical potential on the shape evolution of nanocrystals have been elucidated by Peng et al., and in the case of one-dimensional nanostructure growth it would be advantageous to have a higher chemical potential,[6,7] which is mainly determined by the pH value and monomer concentration of the solutions in our adopted reaction system. Meanwhile, faster ionic motion usually ensures a reversible pathway between the fluid phase (solution, melt, or vapor) and the solid phase, which allows atoms, ions, or molecules to adopt correct positions in developing crystal lattices.[23] Control experiments have been carried out to investigate the influence of monomer concentration and pH value on the growth of $Ln(OH)_3$ nanowires.

The synthesis of colloidal solutions of $Ln(OH)_3$ should be critical in the synthesis of lanthanide hydroxide nanowires. A rapid adjustment of the pH value of the solution leads to the formation of a white precipitate (shown to be aggregates of nanoparticles) which immediately appears in solution. This feeding mode can be regarded as a similar process to the "injection" technique adopted by Peng et al., which will ensure a higher monomer concentration so that the obtained precipitates will have many anisotropic seeds[9] for the following hydrothermal process.

Control experiments have been carried out to investigate the influence of pH value on the morphology of the final products. In the synthesis of $Sm(OH)_3$ nanomaterials, nanosheets are obtained when the pH value of the solution is maintained between 6 and 7 (Figure 4A). These nanosheets are apparently the product of a mixed-shape evolution of 1D and 2D ripening.[6] When the pH value is increased to 9, the obtained $Sm(OH)_3$ material is found to be in the form of uniform nanowires with an aspect ratio of 200–300 (Figure 4B). When the pH value is further increased to 14, or a higher concentration of KOH is employed (to 5 mol L^{-1}), the aspect ratio decreases dramatically to be about 10 (Figure 4C). From the experimental results, it seems that there exists an optimal pH value for the growth of high-aspect-ratio nanowires. This phenomenon can be explained by the complex interaction and balance between the chemical potential and the rate of ionic motion. A higher pH value implies a higher OH^- ion concentration and a higher chemical potential in solution. A high chemical potential is preferable for the growth of nanowires, however, higher OH^- ion concentrations may greatly reduce the Sm^{3+} ion concentration in solution, which is restricted by the value of K_{sp} for $Sm(OH)_3$, and thus reduce the rate of ionic motion. Thus, as the pH value is gradually changed, there must exist a value which is optimal for the preparation of nanowires. The growth behavior must also be closely related to the intrinsic properties of corresponding samples; for example, in the case of $Gd(OH)_3$, nanosheets have not been

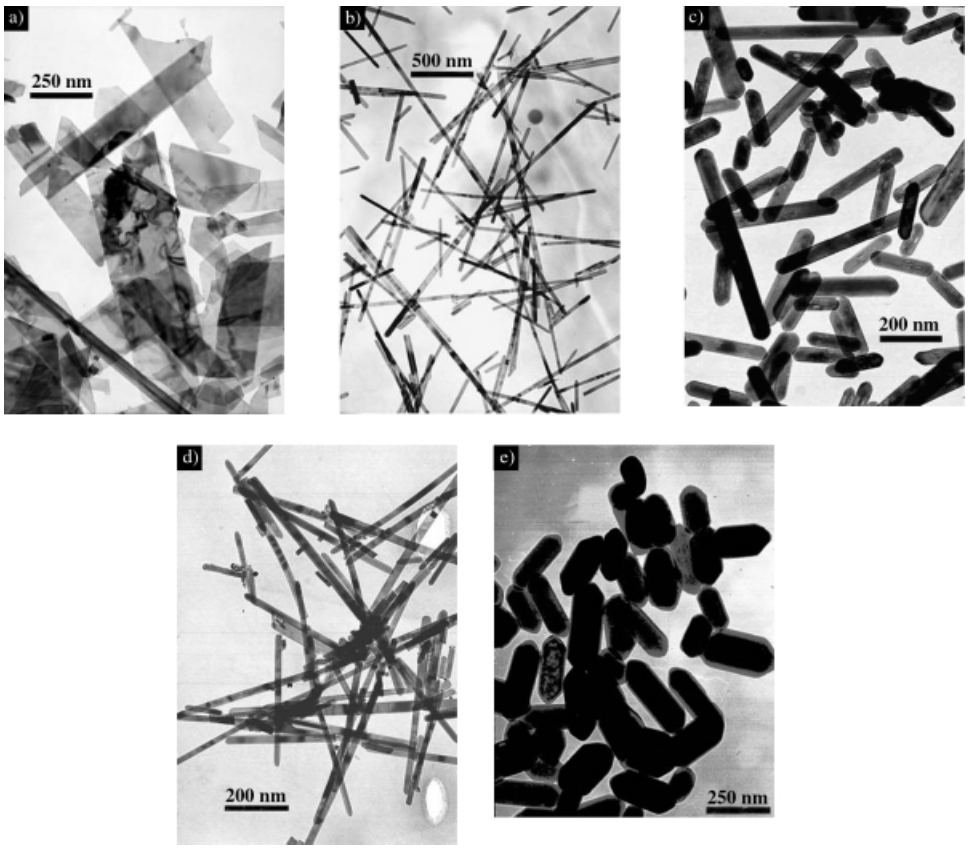

Figure 4. TEM images of: a) $Sm(OH)_3$ nanosheets (pH 6–7); b) $Sm(OH)_3$ nanowires (pH 9–10); c) $Sm(OH)_3$ nanorods (KOH, 5 mol L^{-1}); d) $Gd(OH)_3$ nanowrires, (pH 7); e) $Gd(OH)_3$ nanorods (KOH, 5 mol L^{-1}).

  0044-8249/02/4124-4792 $ 20.00+.50/0 *Angew. Chem. Int. Ed.* **2002**, *41*, No. 24

obtained at lower pH values, although the aspect ratio of the products has been reduced, while at higher pH values, the $Gd(OH)_3$ nanocrystals have a much lower aspect ratio (Figure 4F) than that of the $Sm(OH)_3$ nanorods.

Further investigations can be carried out on the growth dynamics of the family of $Ln(OH)_3$ nanowires, which might serve as a perfect model to study crystallization on the nanoscale, as a trend in their crystal structures can be determined.

As a new material for the synthesis of nanowires, lanthanide hydroxides have many potential applications. The surface hydroxyl groups of $Ln(OH)_3$ may act as active sites for possible surface modification treatment through condensation reactions with amino acids or biologically active molecules, and thus, $Ln(OH)_3$ nanowires may have potential in the field of biological labeling. In addition, the similarity of their crystal structures and lattice constants[24] suggests that doped $Ln(OH)_3$ nanowires could be prepared by a similar growth process, as lattice mismatching would not be a serious concern. Meanwhile, since $Ln(OH)_3$ can be used to prepare oxides or sulfides through dehydration or sulfuration,[24] the $Ln(OH)_3$ or co-doped $Ln(OH)_3$ nanowires may act as important precursors to lanthanide oxide or sulfide nanowires.

In summary, we have developed a facile hydrothermal synthetic method to prepare $Ln(OH)_3$ nanowires that are expected to exhibit some novel properties, and we have displayed the successful synthesis of 1D lanthanide nanostructures, which may lead to new and important opportunities in lanthanide chemistry.

Experimental Section

To prepare lanthanide nanowires, Ln_2O_3 (0.4 g) was dissolved in concentrated nitric acid, and then the solution was rapidly adjusted to a designated pH value using 10% KOH solution. A white precipitate of amorphous $Ln(OH)_3$ appeared immediately. After stirring for about 10 min, the precipitate was then transferred into a 50-ml autoclave, which was filled with deionized water up to 80% of the total volume, sealed, and heated at 180°C for about 12 h. The system was then allowed to cool to room temperature. The final product was collected by filtration, and washed with deionized water to remove any possible ionic remnants, and then dried at 60°C.

The obtained sample was characterized on a Bruker D8-advance X-ray powder diffractometer with $Cu_{K\alpha}$ radiation ($\lambda = 1.5418$ Å). The size and morphology of the $Ln(OH)_3$ nanowires was determined at 200 kV by a Hitachi H-800 transmission electron microscope (TEM) and a JEOL JEM-2010F high-resolution transmission electron microscope.

Received: August 28, 2002 [Z50057]

[1] X. F. Duan, Y. Huang, Y. Cui, J. F. Wang, C. M. Lieber, *Nature* **2001**, *409*, 66 – 69.
[2] W. U. Huynh, J. J. Dittmer, A. P. Alivisatos, *Science* **2002**, *295*, 2425 – 2427.
[3] L. S. Li, J. Walda, L. Manna, A. P. Alivisatos, *Nano Lett.* **2002**, *2*, 557 – 560.
[4] M. H. Huang, S. Mao, H. Feick, H. Q. Yan, Y. Y. Wu, H. Kind, E. Weber, R. Russo, P. D. Yang, *Science* **2001**, *292*, 1897 – 1899.
[5] M. Law, H. Kind, B. Messer, F. Kim, P. D. Yang, *Angew. Chem.* **2002**, *114*, 2511 – 2514; *Angew. Chem. Int. Ed.* **2002**, *41*, 2405 – 2408.
[6] Z. A. Peng, X. G. Peng, *J. Am. Chem. Soc.* **2001**, *123*, 1389 – 1395.
[7] Z. A. Peng, X. G. Peng, *J. Am. Chem. Soc.* **2002**, *124*, 3343 – 3353.
[8] W. W. Yu, X. G. Peng, *Angew. Chem.* **2002**, *114*, 2474 – 2477; *Angew. Chem. Int. Ed.* **2002**, *41*, 2368 – 2371.
[9] Y. G. Sun, B. Gates, B. Mayers, Y. N. Xia, *Nano Lett.* **2002**, *2*, 165 – 168.
[10] X. Wang, Y. D. Li, *J. Am. Chem. Soc.* **2002**, *124*, 2880 – 2881.
[11] Y. D. Li, J. W. Wang, Z. X. Deng, Y. Y. Wu, X. M. Sun, D. P. Yu, P. D. Yang, *J. Am. Chem. Soc.* **2001**, *123*, 9904 – 9905.
[12] J. P. Cotter, J. C. Fitzmaurice, I. P. Parkin, *J. Mater. Chem.* **1994**, *4*, 1603 – 1609.
[13] J. A. Capobianco, F. Vetrone, J. C. Boyer, A. Speghini, M. Bettinelli, *Opt. Mater.* **2002**, *19*, 259 – 268.
[14] M. S. Palmer, M. Neurock, M. M. Olken, *J. Am. Chem. Soc.* **2002**, *124*, 8452 – 8461.
[15] A. H. Peruski, L. H. Johnson, L. F. Peruski, *J. Immunol. Methods* **2002**, *263*, 35 – 41.
[16] M. C. Cassani, Y. K. Gun'ko, P. B. Hitchcock, A. G. Hulkes, A. V. Khvostov, M. F. Lappert, A. V. Protchenko, *J. Organomet. Chem.* **2002**, *647*, 71 – 83.
[17] R. Kempe, H. Noss, T. Irrgang, *J. Organomet. Chem.* **2002**, *647*, 12 – 20.
[18] J. de Jersey, R. B. Martin, *Biochemistry* **1980**, *19*, 1127 – 1132.
[19] J. R. Lakowicz, G. Piszczek, B. P. Maliwal, I. Gryczynski, *ChemPhysChem* **2001**, *4*, 247 – 252.
[20] Y. D. Li, Y. Huang, T. Bai, L. Q. Li, *Inorg. Chem.* **2000**, *39*, 3418 – 3420.
[21] Y. Hasegawa, S. Thongchant, Y. Wada, H. Tanaka, T. Kawai, T. Sakata, H. Mori, S. Yanagida, *Angew. Chem.* **2002**, *114*, 2177 – 2179; *Angew. Chem. Int. Ed.* **2002**, *41*, 2073.
[22] J. W. Stouwdam, F. C. J. M. van Veggel, *Nano Lett.* **2002**, *2*, 733 – 737.
[23] T. J. Trentler, K. M. Hickman, S. C. Goel, A. M. Viano, P. C. Gibbons, W. E. Buhro, *Science* **1995**, *270*, 1791 – 1794.
[24] C. H. Huang, *Rare Earth Coordination Chemistry*, Science Press, Beijing, **1997**, p. 25.

  0044-8249/02/4124-4793 $ 20.00+.50/0